Biosensors and Bioelectronics 58 (2014) 193–199

Contents lists available at ScienceDirect

Biosensors and Bioelectronics

journal homepage: www.elsevier.com/locate/bios

Impedance based detection of pathogenic *E. coli* O157:H7 using a ferrocene-antimicrobial peptide modified biosensor

Yongxin Li [a,b], Rouzbeh Afrasiabi [b], Farkhondeh Fathi [b], Nan Wang [b], Cuili Xiang [b,c], Ryan Love [b], Zhe She [b], Heinz-Bernhard Kraatz [b,*]

[a] Department of Sanitary Chemistry, Public Health School, West China Medical Center, Sichuan University, Chengdu 610044, PR China
[b] Department of Physical and Environmental Sciences, University of Toronto Scarborough, Toronto M1C 1A4, Canada
[c] Department of Material Science and Engineering, Guilin University of Electronic Technology, Guilin 541004, PR China

ARTICLE INFO

Article history:
Received 4 December 2013
Received in revised form
14 February 2014
Accepted 17 February 2014
Available online 25 February 2014

Keywords:
Peptide
E. coli
Ferrocene
Bioconjugate
Peptide
Bioorganometallic

ABSTRACT

Escherichia coli O157:H7 can cause life-threatening gastrointestinal diseases and has been a severe public health problem worldwide in recent years. A novel biosensor for the detection of *E. coli* O157:H7 is described here using a film composed of ferrocene–peptide conjugates, in which the antimicrobial peptide magainin I has been incorporated as the biorecognition element. Electrochemical impedance spectroscopy was employed to investigate the surface characteristics of the newly developed biosensor and to monitor the interactions between the peptide film and the pathogenic bacteria. X-ray photoelectron spectroscopy and time-of-flight secondary ion mass spectrometry (ToF-SIMS) were employed to confirm the immobilization of ferrocene-conjugate onto the gold surface. Non-pathogenic *E. coli* K12, *Staphylococcus epidermidis* and *Bacillus subtilis* were used in this study to evaluate the selectivity of the proposed biosensor. The results have shown the order of the preferential selectivity of the method is *E. coli* O157:H7 > non-pathogenic *E. coli* > gram positive species. The detection of *E. coli* O157:H7 with a sensitivity of 10^3 cfu/mL is enabled by the biosensor. The experimental conditions have been optimized and the plot of changes of charge transfer resistance (ΔR_{CT}) and the logarithm of the cell concentration of *E. coli* O157:H7 shows a linear correlation in the range of 10^3–10^7 cfu/mL with a correlation coefficient of 0.983.

1. Introduction

Escherichia coli (*E. coli*) O157:H7 is one of the most representative serotypes of *Enterohemorrhagic Escherichia coli* (EHEC). It can produce Shiga-like toxin and cause life-threatening gastrointestinal infections, such as bloody diarrhea, hemorrhagic colitis, renal failure and meningitis (Tarr et al., 2000). Since *E. coli* O157:H7 was first reported in the US in 1982, many outbreaks, cases, and deaths associated with the bacteria have occurred with increasing frequency all over the world (Crump et al., 2002; Hrudrey et al., 2003; Bono et al., 2007). *E. coli* O157:H7 contamination is a current major threat to the public health. Therefore, a rapid, inexpensive and sensitive method for the detection of *E. coli* O157:H7 is urgently needed.

Classical identification methods for pathogenic bacteria involves several steps: selective culture, Gram staining, as well as biochemical and/or serological tests. They are still considered as the gold standards for microbiological detection. However, these assays are labor-intensive and often require 4–7 days to obtain a confirmed result for a particular bacterial strain. The use of real-time PCR (Miszczycha et al., 2012), loop-mediated isothermal amplification (Wang et al., 2012), and Pulsed-Field Gel Electrophoresis (Osek and Gallien, 2002) makes it possible to obtain a rapid and sensitive analysis. However, these methods have some drawbacks, such as complexity of primer design and requirement of expensive instruments or reagents.

In recent years, biosensors have played increasingly important roles in pathogenic bacteria detection. Until now, pathogen biosensors mainly include immunosensing and DNA-based detection. A variety of immunosensors have been developed based on the antigenicity of the target bacterial cells, which utilizes fluorescence (Heyduk and Heyduk, 2010), electrochemical impedance (Lu et al., 2013; Barreiros dos Santos et al., 2013; Maalouf et al., 2007), quartz crystalline microbalance (QCM) (Guo et al., 2012), and surface plasmon resonance (SPR) (Maalouf et al., 2007; Baccar et al., 2010). However, the instability of antibodies in harsh environment and the single-use nature of most immunosensors limits the practical application of these biosensors. DNA-based sensors require efficient DNA extraction and some of them need DNA amplification using polymerase chain reaction (PCR) as bacterial cells contain a low copy number of DNA (Liao and Ho, 2009; Heo and Hua, 2009; Yeung et al., 2006). Some other sensors which are

* Corresponding author. Tel.: +1 416 287 7197.
E-mail address: bernie.kraatz@utoronto.ca (H.-B. Kraatz).

http://dx.doi.org/10.1016/j.bios.2014.02.045
0956-5663

based on the detection of β-galactosidase and pH variations have also been reported (Serra et al., 2005; Ercole et al., 2003).

Antimicrobial peptides (AMPs), have the advantages of good stability, simple synthesis procedure, and broad binding affinity towards microorganisms, which enable them particularly promising for pathogenic biosensing applications (Soares et al., 2008). Although the exact mechanisms of antimicrobial peptides for killing the bacteria are not clear, it has been reported that AMPs attach on the bacteria before they lyse the cells. Based on this principle, several biosensors have been developed in the latest years. Kulagina et al. reported two biosensor assays, in which magainin I was chosen as the recognition molecule immobilized on silanized glass slides through direct colvalent conjugation and biotin–advidin chemistry (Kulagina et al., 2005, 2006). These assays for *E. coli* have the detection limits of 1.6×10^5 and 6.8×10^5 cell/mL. Manu S. Mannoor et al. reported an enhanced detection using the biosensor based on magainin I (Mannoor et al., 2010). This work was conducted on interdigitated gold electrodes and the binding activities between the peptide and bacteria were monitored by electrochemical impedance spectroscopy (EIS) and results suggested that magainin I possesses some level of selectivity for bacterial recognition.

Ferrocene (Fc) and its derivatives are often used in electrochemical systems owing to their flavourable electrochemical properties (Martić et al., 2012; Sowole and Kraatz, 2012). So far, no attempt has been made to exploit the use of Fc-conjugates as redox reporters/relays in AMP modified biosensor for the detection of bacteria. In this work, a novel sensor based on magainin I was developed by introducing a Fc label. In addition, EIS method, which can exhibit much higher sensitivity than other conventional counterparts such as amperometric, voltammetric, and potentiometric measurements (Park and Park, 2009), was employed to monitor the binding activity between AMP and bacteria in this study and the measurements were compared to unlabeled magainin I films, which lack the Fc probe. The proposed detection method is rapid, inexpensive, sensitive and therefore attractive for clinic applications as well as environmental analysis.

2. Material and methods

2.1. Preparation of the AMP biosensor

Prior to use, the gold electrode was immersed in piranha containing H_2SO_4 and 30% H_2O_2 (3:1, v/v) for 2 min, polished with 0.3 and 0.05 μm aluminum powder respectively. After thoroughly rinsed with purified water, the electrode was electrochemically cleaned in 0.5 M NaOH, by scanning from −2.0 to 0.1 V (vs Ag/AgCl) at a scan rate of 0.1 V s^{-1}. Then the electrode was immersed in 0.5 M H_2SO_4 and cleaned by running cyclic voltammetry (CV) in the range of 0–1.5 V until a stable gold oxidation peak at 1.1 V was obtained.

The freshly cleaned electrode was immersed in absolute ethanol and sonicated for 5 min and blown dried with nitrogen gas. The gold electrode was then incubated with 2 mM lipoic acid NHS for 2 days at 4 °C to form a self-assembled monolayer (SAM), followed by incubation in 2 mM Fc derivative solution for 24 h at room temperature. To immobilize the antimicrobial peptide, the terminal carboxylic groups of the surface were activated by incubation in the mixture of 10 mM EDC and 10 mM NHS for 2 h at room temperature. Subsequently, the gold electrodes were incubated with 0.4 mM antimicrobial peptide in 10 mM PBS, pH ~ 7.4, overnight at 4 °C. After the immobilization of antimicrobial peptide, the electrodes were rinsed with ultrapure water and blocked by immersing in 100 mM ethanolamine for 1 h, followed by 1 mM hexanethiol for 10 min to back-bill the exposed spots of gold surfaces. Finally, the electrode was rinsed with 10 mM phosphate buffer solution to obtain the AMP-modified sensor surface. The schematic diagram of surface modification and preparation of biosensor electrode is shown in Fig. 1.

2.2. Bacterial culture conditions and detection

The bacteria were incubated with shaking at 200 rpm for 24 h in LB (Luria Bertani) broth at 37 °C. The cells were harvested and killed with 4% PFA, then washed for several times with 10 mM PBS solution (pH = 7.4). Optical density at 600 nm (OD_{600}) was measured and adjusted to around 0.60, corresponding to bacteria concentration of 10^8 colony forming units (cfu) /mL.

AMP modified gold electrodes were incubated in the bacterial cell suspensions in 10 mmol/L PBS buffer (pH = 7.4) for 1.5 h at 37 °C. Then the electrodes were rinsed thoroughly using 10 mM PBS (pH = 7.4) to remove unbound bacterial cells and then characterized by EIS.

2.3. Electrochemical measurements

The electrochemical experiments were carried out in an enclosed faraday cage with a three-electrode system, including the AMP modified gold electrode as the working electrode, Pt wire as the counter electrode, and Ag/AgCl/3.0 M KCl as the reference electrode. A salt bridge filled with agar and KNO_3 was employed to minimize the transfer of chloride ions from the reference electrode to the measurement system. The electrochemical measurements were performed in 10 mM phosphate buffer (pH ~ 7.4), containing 5 mM/5 mM $K_3[Fe(CN)_6]/K_4[Fe(CN)_6]$ as the redox probe. EIS experiments were conducted in the frequency range of 100 kHz to 0.1 Hz with AC amplitude of 5 mV, at the formal potential of the redox probe $[Fe(CN)_6]^{3-/4-}$ (0.25 V vs Ag/AgCl). The ZSimpWin 2.0 software was used to analyze the EIS data, which was represented as Nyquist

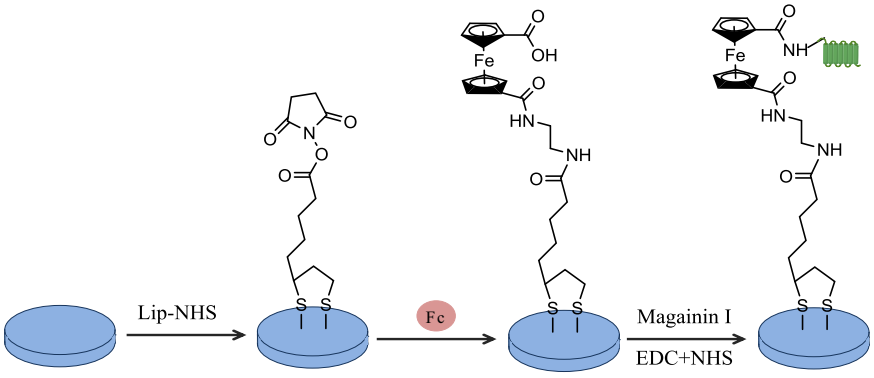

Fig. 1. Schematic diagram for the construction of ferrocene–peptide-modified biosensor.

plots using the real impedance Z_{re} and the imaginary part Z_{im}. Differential pulse voltammetry (DPV) experiments were carried out in the range from 0 to 700 mV with a step potential of 4 mV, amplitude of 50 mV, and a frequency of 25 Hz. All the measurements were repeated at least three times to obtain statistically meaningful results.

2.4. XPS and TOF-SIMS analyses

Surface preparation: Au coated Si wafers (100 nm Au on 7 nm Ti adhesion layer on Si) were cleaned with piranha solution for 2 min, rinsed and then sonicated in absolute ethanol and Millipore water for 10 min, respectively. After drying with N_2, the clean surface was incubated with 2 mM lipoic acid NHS for 2 days at 4 °C, followed by a 2 mM solution of Fc–magainin for 24 h at room temperature. Prior to analysis, the wafer surface was thoroughly rinsed with ethanol and dried with a stream of N_2.

The XPS analyses were performed with an Al-Kα X-ray source (15 mA, 14 kV). The operating pressure was 1×10^{-10} Torr and the take-off angles from the surface were 30°, 50°, and 70°. The XPS spectra were obtained with a pass energy of 200 eV for the survey scan and a pass energy of 10 eV for the S 2p region. The binding energies were calibrated using Au 4f7 at 84.0 eV.

On the other hand, TOF-SIMS measurements were conducted using TOF-SIMS IV (ION-TOF GmbH, Germany) with a Bi liquid metal ion source. A Bi^{3+} primary beam was employed. The cycle time for the bombardment process and detection was 100 μs. For each sample, positive and negative ion modes for each sample were analyzed from 128pixel × 128 pixel over an area of 500 × 500 μm^2 for 100 s.

3. Results and discussion

3.1. Characterization of the AMP biosensor

Electrochemical impedance spectroscopy is an effective method to investigate surface modification. Fig. 2 illustrates the representative Nyquist plots of the impedance spectra for different modified surfaces in the presence of the redox probe of $[Fe(CN)_6]^{3-/4-}$. A modified Randles equivalent circuit was selected to represent the electrochemical process at the electrodes. This model contains four circuit elements, including the solution phase resistance R_S, the charge transfer resistance R_{CT}, the Warburg impedance W, and the constant phase element Q. Among them, R_S and Z_W reflect the resistance of the supporting electrolyte and the diffusion properties of the redox probe in the solution, respectively. CPE corresponds to a nonlinear capacitor accounting for the inhomogeneity of the formed film. The semicircle diameter of the Nyquist diagram corresponds to the charge transfer resistance R_{CT}, which is the most important parameter and determined by the dielectric and insulating properties of the surface layer. The modification and interaction with analytes on the surface can lead to the change in the R_{CT} value.

As shown in Fig. 2, the bare gold electrode exhibited an extremely small semicircle diameter, which implied that charge transfer easily happened on the bare gold surface. Immobilization of lipoic acid-NHS ester on the gold surface led to a significant increase of the semicircle diameter. R_{CT} increased greatly from 6.1 to 4047 Ω cm^2. This indicated that film formation prevented the diffusion of the redox probe into the film to some extent. The conjugation of Fc derivative made the diameter of the semicircle diameter decrease (R_{CT} decreased to 544 Ω cm^2). This is not surprising, since the Fc derivative facilitates charge transfer. Then, a further increase in the semicircle diameter was observed and the R_{CT} value increased to 11,650 Ω cm^2. This increase is due to the attachment of the N-terminal of AMP to the activated carboxyl group of the Fc derivative, which increased film thickness. The R_{CT} value dramatically increased to 17,570 Ω cm^2 after surface back-filling with hexanethiol. In addition, the impedance spectrum showed an absence of the low frequency loop, Z_W, because the potential pinholes of the electrode surface were occupied, which resulted in a higher interfacial resistance to ion.

In order to confirm the conjugation of Fc, DPV measurements were carried out for the electrodes modified by lipoic acid-NHS ester and by lipoic acid NHS+Fc, respectively. As shown in Fig.S3 (Supporting information), an obvious peak at 0.47 V was present in DPV spectrum obtained from the surface modified by lipoic NHS+Fc, which proved Fc successfully immobilized onto the surface.

3.2. XPS and ToF-SIMS analyses

X-ray photoelectron spectroscopy (XPS) and Time-of-flight secondary ion mass spectrometry (ToF-SIMS) are two of the important surface analysis techniques. In this study, XPS and ToF-SIMS were employed to further confirm the surface immobilized by Lipoic acid-NHS+Fc on the silicon wafer. The modification was conducted on silicon wafer using the same procedure with gold electrode.

From the XPS survey scan, the presence of S, C, O, N and Fe peaks initially revealed that the modified surface contained the elementary composition of lipoic acid-NHS and Fc (Fig. 3). A significant S coverage with two peaks at 162.76 eV and 163.95 eV was observed in the high-resolution XPS of S 2p (Fig. 3a). The first doublet corresponds to the S 2p3/2 peak assigned to the S atoms of lipoic acid-NHS bound to the gold

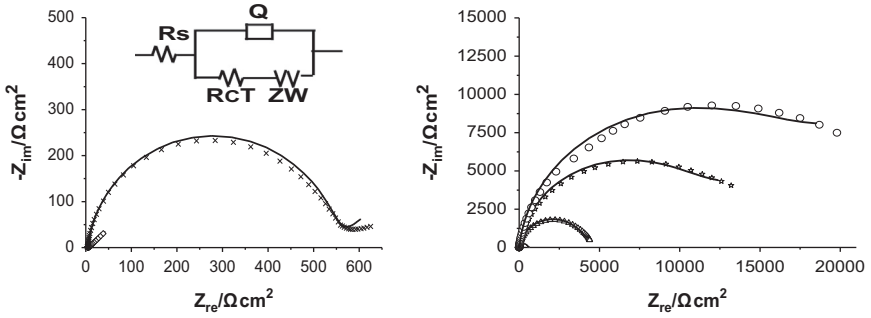

Fig. 2. Impedance spectra of the surface after each modification step: (□) bare gold; (Δ) after coating with lipoic NHS; (×) after immobilization of Fc; (☆) after covalent binding of the AMP; and (○) after back-filling with hexanethiol. The impedance spectra were recorded from 100 KHz to 0.1 Hz. Experimental data are shown as points and calculated results correspond to solid lines. Impedance spectra were obtained in the presence of the redox probe, at a formal potential of 250 mV vs Ag/AgCl, and AC amplitude of 10 mV. The inset shows the equivalent circuit model: R_S is the solution resistance, Q is the constant phase elements, R_{CT} is the charge transfer resistance, and Z_W is the finite length Warburg impedance.

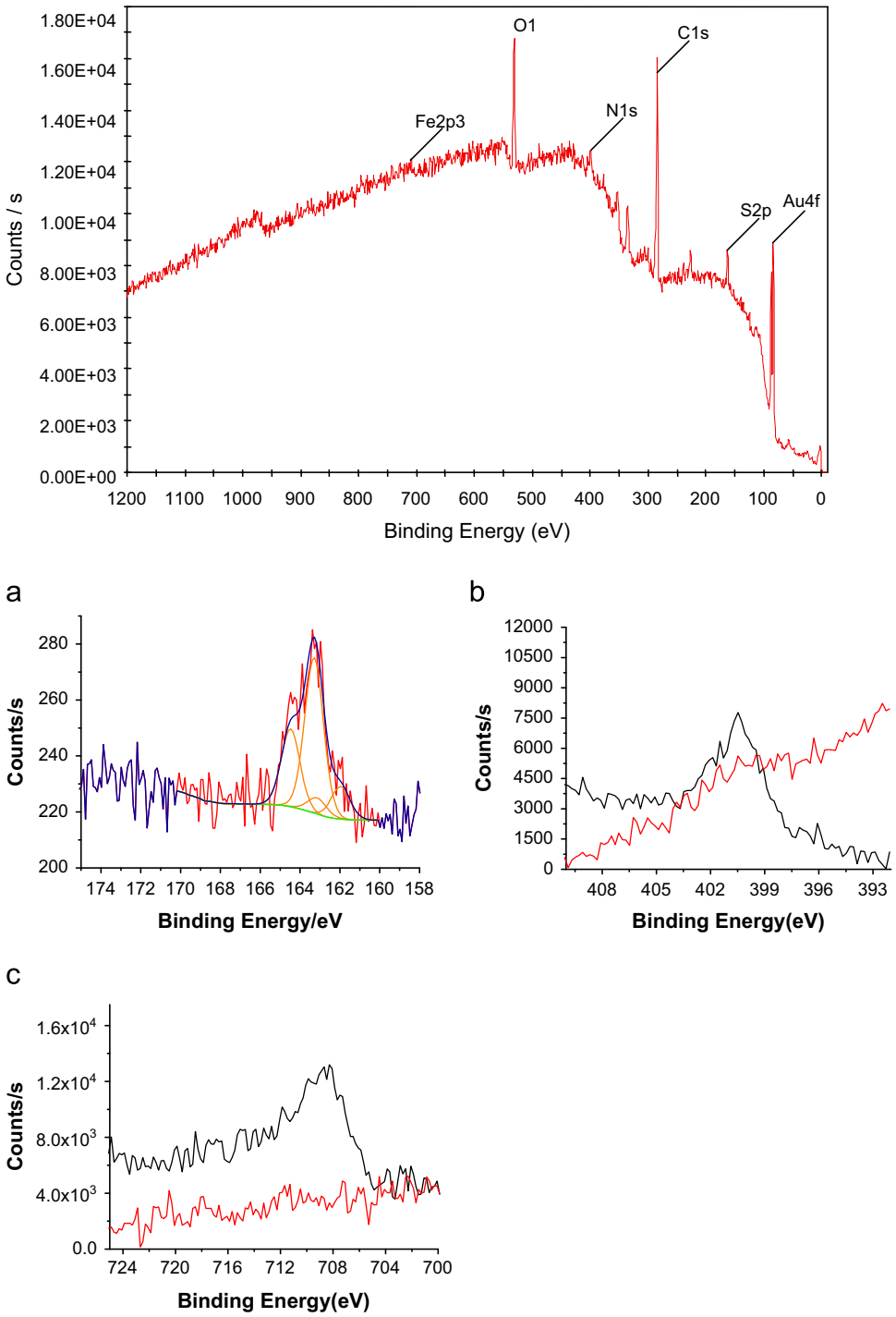

Fig. 3. XPS spectra of the gold surface modified by lipoic NHS+Fc. (a) High-resolution XPS of S 2p peaks, (b) 2-scan XPS spectra of N 1s, and (c) 10-scan XPS spectra of Fe 2p3. The red line indicates the surface modified by lipoic NHS and the black line indicates the surface after the Fc conjugation. (For interpretation of the references to color in this figure legend, the reader is referred to the web version of this article.)

surface by Au–S bond, whereas the second peak represents the S 2p1/2 peak indicating a physisorbed moiety (Labib et al., 2011) In addition, the scan XPS spectra at N 1s region showed a N peak at 400.6 eV on the surface after Fc conjugation, indicating the presence of amides due to the introduction of Fc derivative (Fig. 3b) (Briand et al., 2006; Wirde and Gelius, 1999). Finally, a 10-scan XPS spectra of Fe showed a Fe 2p3/2 peak at 709.4 eV only on the surface after Fc conjugation, indicating Fc containing Fe(II) was immobilized on the surface (Fig. 3c).

In addition, ToF-SIMS studies were carried out to get additional information about the Fc–peptide films on the the gold surface. The ToF-SIMS spectra showed a high AuS^- fragment ion intensity at $m/z=228.94$ in the negative mode (Fig. 4a). We compared the Fe ion intensities of films of magainin I and of Fc–magainin I and found the presence of a significant Fe^+ peak (at $m/z=55.92$) only for the Fc-labeled film (Fig. 4b).

3.3. Incubation time

EIS was employed to monitor the binding activity between AMP and bacteria in this study. We investigated the influence of different incubation time ranging from 15 min to 1.5 h on the

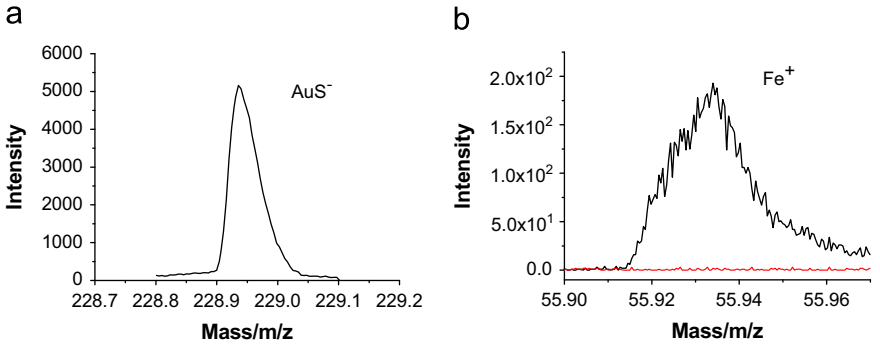

Fig. 4. ToF-SIMS spectra of the gold surface modified by lipoic NHS+Fc. (a) AuS^-, and (b) Fe^+. The base line is the response after surface modification by lipoid NHS. After Fc conjugation a strong signal for Fe^+ is observed.

attachment of bacteria onto the AMP surface. As shown in Fig. S4 (Supporting information), we did not observe any significant change in the impedance until the incubation time was more than 15 min. A considerable decrease of impedance was observed after 1.5 h of contact between *E. coli* O157:H7 and the gold surfaces, which indicated that more bacteria attached to the surfaces due to a longer contact time. This finding was in agreement with the findings by Humblot et al. (2009). Cell membranes of bacteria are insulating. Thus binding of cells to a surface are expected to result in an increase of the impedance response. In case of the label-free assay, binding of bacterial cells to the magainin I film significantly reduces the electron transfer between the ferri/ferrocyanide redox probe in solution and the electrode surface, resulting in an increased R_{CT}. However, in case of the Fc–magainin I film, in the absence of the target bacteria *E.coli* O157:H7, a larger impedance was observed, presumably due to better packing at the peptide/solution interface. Upon binding of the bacteria to the Fc–peptide film, structural changes may be larger, which can expose the Fc group to the solution. It may be speculated that upon binding of target bacteria to the AMP surface, the membrane interface promotes the formation of an amphipathic helix that orientated at the interface of bacterial cell membrane (Lad et al., 2007) and thus the Fc group is more accessible to the solution-based redox probe, resulting in a more significant decrease in R_{CT}, thereby changing the sensing parameter ΔR_{CT} to a larger extent.

3.4. Selectivity of the AMP-biosensor

The binding activity of AMP surfaces was tested using non-pathogenic *E. coli* K12, and two Gram-positive bacteria (*Staphylococcus epidermidis* and *Bacillus subtilis*) in order to assess the selectivity of the developed biosensor. As shown in Fig. 5, that 10^7 cfu/mL of *S. epidermidis* and *B. subtilis* caused a slight decrease in the impedance when compared to the blank. 10^7 cfu/mL of *E. coli* K12 showed a relatively obvious impedance decrease, which was less than the impedance change caused by 10^4 cfu/mL of *E. coli* O157:H7. The results showed the functionalized biosensor exhibited preferential binding for different bacteria as followed: *E. coli* O157 > *E. coli* K12 > *S. epidermidis* and *B. subtilis*.

Although the antibacterial mechanisms of magainin I has not been clear, the previous reports support that electrostatic attraction is the prerequisite of cationic AMP selective binding on bacterial membrane (Yu et al., 2008; Bessalle et al., 1992). From the results, it is evident that there exists a remarkable difference of the selectivity of magainin I between Gram-positive and Gram-negative bacteria. This may be associated with the different structure of their cell walls. The cell walls of Gram-negative bacteria consist of an outer membrane located above a thin peptidoglycan layer, which contain lipopolysaccharides (LPS) with negative charges. Thus, the electrostatic attraction assists initially

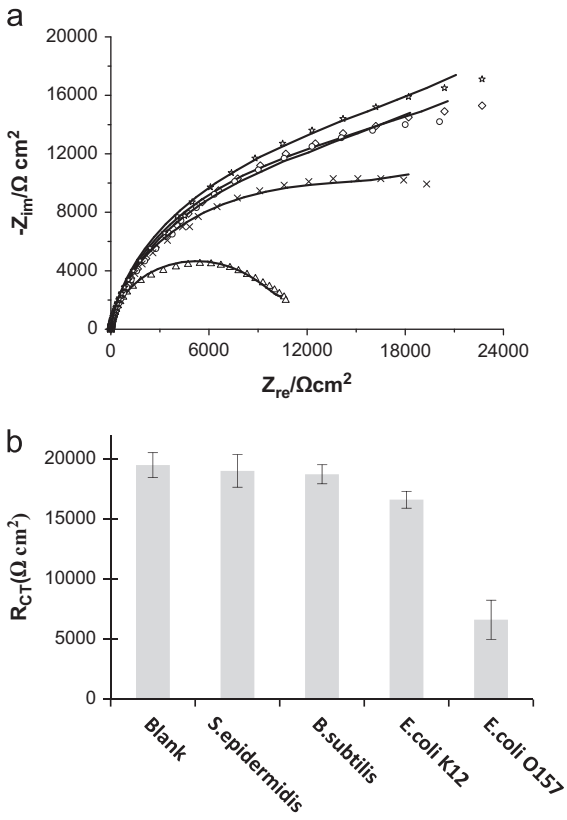

Fig. 5. Impedance spectra of the selectivity of AMP modified biosensor towards different bacteria. (a) Impedance spectra of the AMP modified biosensor after incubation in different bacteria (10^7 cfu/mL). (☆)back-filling, (□)*S. epidermidis*,(○)*B. subtilis*, (×) *E. coli* K12, (Δ)*E. coli* O157. The impedance were recorded from 100 KHz to 0.1 Hz. Measured data is shown as symbols with calculated fit to the equivalent circuit as solid lines. Impedance spectra obtained in phosphate buffer (pH ~ 7.4), containing 5 mM/5 mM $[Fe(CN)_6]^{3-/4-}$ as the redox probe, at a formal potential of 250 mV vs Ag/AgCl, and ac amplitude of 10 mV. (b) Impedance changes caused by different bacterial species. Error bars represent the standard deviation for triplicate measurements.

cationic magainin I binding with the anionic LPS on the Gram-negative cell surface. By contrast, the cell walls of Gram-positive bacteria have a thicker peptidoglycan layer and teichoic acids instead of the anionic LPS (Beveridge, 1999). In the recent study, weak binding was found between magainin I and Gram positive bacteria, which may be a consequence of the teichoic acids in Gram positive bacteria with a small amount of negative charges. In addition, the LPS of *E. coli* O157:H7 contain O antigen and H antigen, which are hydrophilic branched sugar side chains and may increase electrostatic and hydrogen bonding with maganin I (Mannoor et al., 2010) *E. coli* K12 strains lack O antigen, so they

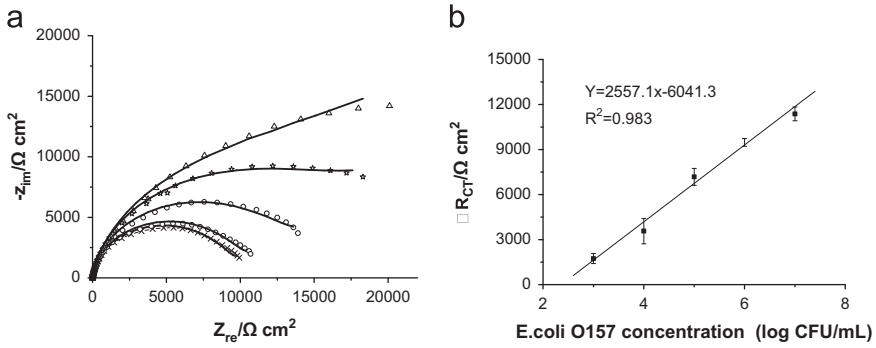

Fig. 6. Electrochemical impedance spectra of AMP biosensor for different *E. coli* O157:H7 concentrations. (△) 10^3 cfu/ml, (☆) 10^4 cfu/ml, (○) 10^5 cfu/ml blank, (□) 10^6 cfu/ml, and (×) 10^7 cfu/ml. The impedance were recorded from 100 KHz to 0.1 Hz. Experimental data are shown as points and calculated results correspond to solid lines. Impedance spectra obtained in presence of a redox probe, at a formal potential of 250 mV vs Ag/AgCl, and ac amplitude of 10 mV. (b) Variation of the charge transfer resistance (ΔR_{CT}) vs log (*E. coli* concentration) calculated according to the equivalent circuit ($\Delta R_{CT}=R_{CT}$(back-filling)$-R_{CT}$(after binding)).

provide a good comparison to *E. coli* O157:H7. Hence, the magainin I modified surface preferentially bind pathogenic G−bacteria vs nonpathogenic strains of *E. coli* and G+bacteria.

3.5. The sensitivity measurements of the method

To evaluate the sensitivity of the method, the developed AMP biosensor was employed to test the *E. coli* O157:H7 suspensions of tenfold serial dilution. The adhesion of *E. coli* O157:H7 cells were monitored as a decrease in R_{CT} by EIS. The attempts of quantitative detection of *E. coli* O157 were made using the proposed biosensor. As shown in Fig. 6, a decrease of the diameters of the semicircles could be observed with the *E. coli* O157:H7 concentrations increasing. It might be caused by the fact that more binding between AMP and *E. coli* O157:H7 led to more severe distortion in the film, which made the charge transfer to the gold surface more easily and a decrease of R_{CT} was obtained. At a cell concentration of 10^7 cfu/mL, the change in R_{CT} is comparatively insensitive to changes in the cell concentration, probably due to surface saturation. Under the optimized experimental conditions, the changes in charge transfer resistance ($\Delta R_{CT}=R_{CT}$(back-filling)$-R_{CT}$(after binding)) increased continuously as bacteria concentrations increasing. The ΔR_{CT} and the logarithm of the cell concentration showed a linear correlation in the range of 10^3–10^7 cfu/mL. The linear equation was expressed as: $\Delta R_{CT}=2557.1 \log C - 6041.3$, where ΔR_{CT} denotes the change of charge transfer resistance, C denotes the cell concentration of *E. coli* O157:H7. The correlation coefficient was 0.983. The sensitivity of the method was as low as 10^3 cfu/mL, which was comparable with or better than the detection limit of pathogenic *E. coli* by most developed impedance sensors (Varshney and Li, 2007; Escamilla-Gómez et al., 2009; Dweik et al., 2012; Chan et al., 2013; Basu et al., 2014). The whole detection took less than 2 h to perform.

With regard to cationic AMPs as recognition molecules in biosensors, the detection sensitivity may be affected by different conjugation approaches of the peptides. Soares et al. reported that modification of the N-terminal of the AMP reduced the antimicrobial activity greatly, while substitutions within the C-terminus had no significant effect on the potency (Soares et al., 2008). This was contrast to Besalle, who reported that removal of the first three amino acids from N-terminal end of magainin-2 did not disturb its antibacterial activity (Zasloff et al., 1988) In addition, Kulagina et al. reported that the detection limit for *E. coli* with N-terminal immobilized magainin I was at least four-fold lower than the surfaces where magainin I was immobilized *via* C-teminal biotin (Kulagina et al., 2005). In the present study, the amine group of Magainin I was covalently bound to the activated carboxyl acid groups of Fc and yet we still obtained a detection limit of 10^3 cfu/mL for *E. coli* O157:H7. This is probably explained by the following two reasons: (1) By looking at the magainin I chemical structure, we know it has one amine group on its N-terminal and four amine groups of lysine on its lateral chains for every molecule. In neutral pH, magainin I carries a net charge of +3 (Khandelia et al., 2008). The activated carboxyl groups of Fc only react with the deprotonated amine groups. Therefore, N-terminal conjugation will not decrease the net positive charges on the surface, thus it will not obviously affect the electrostatic interaction with an anionic bacterial membrane; (2) Additionally, magainin I has five amine groups and exhibits randomly distributed charged residues in solution (random coil). As a result, there are probably different amine immobilization sites on magainin I, and magainin I may have conjugated onto the surface by a lysine residue near C-terminus, which may not interfere with its binding activity.

3.6. Comparision to the detection of label-free biosensor

At the same time, we constructed the label-free biosensor using magainin I. The electrochemical spectra of CV and EIS were showed in Figs. S5 and S6 (Supporting information). The label-free biosensors were used to detect *E. coli* O157:H7 suspensions of different concentrations (Fig. S7). As expected, here bacteria binding was accompanied by a dramatic increase in impedance unlike the results observed with Fc labeled sensor. In addition, the impedances increased as the cell concentrations increased. This label-free biosensor achieved a detection limit of 10^4 cfu/mL *E. coli* O157:H7, which was one order of magnitude higher than the Fc labeled biosensor.

4. Conclusions

The rapid detection of *E. coli* O157:H7 by an electrochemical sensor employing a ferrocene–peptide conjugate was demonstrated in this study. The response characteristics of the sensor were thoroughly investigated by electrochemical impedance spectroscopy and compared to peptide films that lack the ferrocene label. It is shown that this biosensor can sense the concentration of *E. coli* O157:H7 down to 10^3 cfu/mL, which represents an increase in detection limit by a factor of 10 compared to the label free biosensor, which possesses only the recognition element magainin I but lacks the ferrocene label. In addition, the selectivity of the electrochemical sensor was evaluated using a series of bacteria. The difference from using immunosensing and DNA based sensors targeting the known pathogenic species is that the use of antibacterial peptides as recognition element for sensors is a novel

technique that potential may find a wide range of applications for the detection of a wide range of Gram+/− pathogens.

Acknowledgments

We appreciate funding from NSERC and from the University of Toronto. Y.L. and C.X. were supported by the Visiting Scholars Program. In addition, we are grateful to the following individuals for their help with XPS and TOF-SIMS (Dr. Rana Sodhi of the Surface Interface Ontario center at University of Toronto), with bacteria (Dr. Mauricio R. Terebiznik, Department of Cell & System Biology at the University of Toronto Scarborough).

Appendix A. Supplementary material

Supplementary data associated with this article can be found in the online version at http://dx.doi.org/10.1016/j.bios.2014.02.045.

References

Baccar, H., Mejri, M.B., Hafaiedh, I., Ktari, T., Aouni, M., Abdelghani, A., 2010. Talanta 82, 810–814.
Barreiros dos Santos, M., Agusil, J.P., Prieto-Simón, B., Sporer, C., Teixeira, V., Samitier, J., 2013. Biosens. Bioelectron. 45, 174–180.
Basu, P.K., Indukuri, D., Keshavan, S., Navratna, V., Vanjari, S.R.K., Raghavan, S., Bhat, N., 2014. Sens.Actuators B 190, 342–347.
Bessalle, R., Haas, H., Goria, A., Shallt, I., Fridkini, M., 1992. Antimicrob. Agents Chemother. 36, 313–317.
Beveridge, T.J., 1999. J. Bacteriol. 181, 4725–4733.
Bono, J.L., Keen, J.E., Clawson, M.L., Durso, L.M., Heaton, M.P., Laegreid, W.W., 2007. BMC Infect. Dis. 7, 98.
Briand, E., Salmain, M., Compère, C., Pradier, C.M., 2006. Colloids Surf. B Biointerfaces 53, 215–224.
Chan, K.Y., Ye, W.W., Zhang, Y., Xiao, L.D., Leung, P.H., Li, Y., Yang, M., 2013. Biosens. Bioelectron. 41, 532–537.
Crump, J.A., Sulka, A.C., Langer, A.J., Schaben, C., Crielly, A.S., Gage, R., Baysinger, M., Moll, M., Withers, G., Toney, D.M., Hunter, S.B., Hoekstra, R.M., Wong, S.K., Griffin, P.M., Van Gilder, T.J., 2002. N. Engl. J. Med. 347, 555–560.
Dweik, M., Stringer, R.C., Dastider, S.G., Wu, Y., Almasri, M., Barizuddin, S., 2012. Talanta 94, 84–89.
Ercole, C., Del Gallo, M., Mosiello, L., Baccella, S., Lepidi, A., 2003. Sens. Actuators B 91, 163–168.
Escamilla-Gómez, V., Campuzano, S., Pedrero, M., Pingarrón, J.M., 2009. Biosens. Bioelectron. 24, 3365–3371.
Guo, X., Lin, C.S., Chen, S.H., Ye, R., Wu, V.C., 2012. Biosens. Bioelectron. 38, 177–183.
Heo, J., Hua, S.Z., 2009. Sensors (Basel) 9, 4483–4502.
Heyduk, E., Heyduk, T., 2010. Anal. Biochem. 396, 298–303.
Hrudrey, S.E., Payment, P., Hych, P.M., Gillham, R.W., Hrudey, E.J., 2003. Water Sci. Technol. 47, 7–10.
Humblot, V., Yala, J.F., Thebault, P., Boukerma, K., Héquet, A., Berjeaud, J.M., Pradier, C.M., 2009. Biomaterials 30, 3503–3512.
Khandelia, H., Ipsen, J.H., Mouritsen, O.G., 2008. Biochim. Biophys. Acta 1778, 1528–1536.
Kulagina, N.V., Lassman, M.E., Ligler, F.S., Taitt, C.R., 2005. Anal. Chem. 77, 6504–6508.
Kulagina, N.V., Shaffer, K.M., Anderson, G.P., Ligler, F.S., Taitt, C.R., 2006. Anal. Chim. Acta 575, 9–15.
Labib, M., Shipman, P.O., Martic, S., Kraatz, H.B., 2011. Analyst 136, 708–715.
Lad, M.D., Birembaut, F., Clifton, L.A., Frazier, R.A., Webster, J.R., Green, R.J., 2007. Biophys. J. 92, 3575–3586.
Liao, W.C., Ho, J.A., 2009. Anal. Chem. 81, 2470–2476.
Lu, L., Chee, G., Yamada, K., Jun, S., 2013. Biosens. Bioelectron. 42, 492–495.
Maalouf, R., Fournier-Wirth, C., Coste, J., Chebib, H., Saïkali, Y., Vittori, O., Errachid, A., Cloarec, J.P., Martelet, C., Jaffrezic-Renault, N., 2007. Anal. Chem. 79, 4879–4886.
Mannoor, M.S., Zhang, S., Link, A.J., McAlpine, M.C., 2010. Proc. Nat. Acad. Sci. USA. 107, 19207–19212.
Martić, S., Beheshti, S., Rains, M.K., Kraatz, H.B., 2012. Analyst 137, 2042–2046.
Miszczycha, S.D., Ganet, S., Duniere, L., Rozand, C., Loukiadis, E., Thevenot-Sergentet, D., 2012. J. Food Prot. 75, 1373–1381.
Osek, J., Gallien, P., 2002. Vet. Med.—Czech 47, 149–158.
Park, J.Y., Park, S.M., 2009. Sensors 9, 9513–9532.
Serra, B., Morales, M.D., Zhang, J., Reviejo, A.J., Hall, E.H., Pingarron, J.M., 2005. Anal. Chem. 77, 8115–8121.
Soares, J.W., Kirby, R., Morin, K.M., Mello, C.M., 2008. Protein Pept. Lett. 15, 1086–1093.
Sowole, M.A., Kraatz, H.B., 2012. Analyst 137, 1120–1124.
Tarr, P.I., Bilge, S.S., Vary, J.C.J., Jelacic, S., Habeeb, R.L., Ward, T.R., Baylor, M.R., Besser, T.E., 2000. Infect. Immun. 68, 1400–1407.
Varshney, M., Li, Y., 2007. Biosens. Bioelectron. 22, 2408–2414.
Wang, F., Jiang, L., Ge, B., 2012. J. Clin. Microbiol. 50, 91–97.
Wirde, M., Gelius, U., 1999. Langmuir 15, 6370–6378.
Yeung, S.W., Lee, T.M.H., Cai, H., Hsing, I.M., 2006. Nucleic Acids Res. 34, e118.
Yu, L., Ding, J.L., Ho, B., Feng, S., Wohland, T., 2008. Open Chem. Phys. J. 1, 62–79.
Zasloff, M., Martin, B., Chen, H.C., 1988. Proc. Natl. Acad. Sci. USA 85, 910–913.